



1 **PM_{2.5} Source Apportionment Using Organic Marker-based CMB**
2 **Modeling: Influence of Inorganic Markers and Sensitivity to Source**
3 **Profiles**

4
5 **Yingze Tian¹, Xiaoning Wang¹, Peng Zhao¹, Zongbo Shi², Roy M. Harrison^{*2a}**

6
7 ¹ State Environmental Protection Key Laboratory of Urban Ambient Air Particulate Matter Pollution
8 Prevention and Control, College of Environmental Science and Engineering, Nankai University,
9 Tianjin, 300071, China

10
11 ² School of Geography Earth and Environmental Science, University of Birmingham, Edgbaston,
12 Birmingham, B15 2TT, UK

13
14 Corresponding author: Roy M. Harrison (r.m.harrison@bham.ac.uk)

15 ^a Also at: Department of Environmental Sciences / Center of Excellence in Environmental Studies,
16 King Abdulaziz University, PO Box 80203, Jeddah, 21589, Saudi Arabia

17

18



19 **ABSTRACT**

20 Chemical mass balance (CMB) is one of the most popular methods to apportion the sources of PM_{2.5}.
21 However, the source apportionment results are dependent on the choices of measured chemical
22 species and the source profiles. Here, we explore the sensitivity of CMB results to source profiles by
23 comparing CMB modeling based on organic markers only (OM-CMB) with a combination of organic
24 and inorganic markers (IOM-CMB), using organic and inorganic markers in PM_{2.5} samples collected
25 in the Chinese megacity of Chengdu. OM-CMB results show that gasoline vehicles, diesel vehicles,
26 industrial coal combustion, resuspended dust, biomass burning, cooking, vegetation detritus, SOA,
27 sulphate, and nitrate contributed to 4%, 10%, 15%, 12%, 5%, 3%, 4%, 9%, 10%, and 20%, in
28 comparison to 4%, 11%, 15%, 17%, 6%, 2%, 5%, 10%, 7%, and 18% from IOM-CMB modelling.
29 The temporal variations of PM_{2.5} contributions from sulphate, nitrate, SOA, gasoline vehicles, and
30 biomass burning, characterized by unique markers and low collinearity, were in good agreement
31 between the OM-CMB and IOM-CMB results. However, resuspended dust estimates from OM-CMB
32 had a poor correlation with that from IOM-CMB, due to the different tracers used. When replacing
33 the source profile for industrial coal combustion with that for residential sources, the
34 contributions of resuspended dust and residential coal combustion were overestimated because the
35 residential coal combustion profile contained a higher concentration of OC and organic compounds
36 but lower crustal elements. Different source profiles for gasoline vehicles were also evaluated. Our
37 results confirm the superiority of combining inorganic and organic tracers and using up-to-date
38 locally-relevant source profiles in source apportionment of PM.

39

40 **Keywords:** particulate matter, source apportionment, CMB model, organic marker

41



42 **1. INTRODUCTION**

43 Atmospheric fine particles (PM_{2.5}) have long been shown to have pronounced effects on human health
44 (Bell et al., 2014; Yang et al., 2019; Hong et al., 2021; Li et al., 2022; Wen et al., 2022). PM_{2.5} control
45 is a challenging problem, especially in megacities where large populations are exposed to high
46 concentrations. The information on the impacting sources can play an important role in designing
47 effective PM_{2.5} reduction strategies. Many studies have estimated the potential source contributions
48 to PM_{2.5} in megacities using various methods, such as receptor models (Lu et al., 2018; Wang et al.,
49 2013; Perrone et al., 2012; Mor et al., 2021; Song et al., 2021; Zhang et al., 2021a), and air quality
50 models (Clappier et al., 2015; Zhang et al., 2017; Li et al., 2020a; Guan et al., 2021). Among the
51 receptor models, the chemical mass balance (CMB) model approach has been used for source
52 apportionment of PM at many locations, worldwide (Zheng et al., 2002; Perrone et al., 2012; Yin et
53 al., 2015; Chen et al., 2015; Lu et al., 2018; Wu et al., 2020; Wong et al., 2021). This model has some
54 underlying challenges posed by possible collinearity of source profiles, and relevance of source
55 profiles.

56

57 PM_{2.5} is comprised of a complex mixture of chemical components, including both inorganic and
58 organic components. As a significant constituent of PM_{2.5}, organic matter (OM) is comprised of
59 thousands of compounds which show distinctive physical and chemical properties (Zhang et al., 2013;
60 Zhao et al., 2013; Li et al., 2020b; Cao et al., 2021; Li et al., 2021). Generally, the OM is composed
61 of primary organic matter (POM) which is directly emitted, and secondary organic matter (SOM)
62 which is formed through the chemical oxidation of volatile organic compounds (VOCs) (Yang et al.,
63 2016; Zhan et al., 2021; Zhang et al., 2021b). Numerous studies on PM_{2.5} source apportionment have
64 been conducted based upon inorganic markers and OC (Olson et al., 2008; Li et al., 2020c). However,



65 many important PM_{2.5} emission sources (such as cooking) do not have a unique composition (Zhao
66 et al., 2015). Some organic compounds are more specific to individual PM sources and have been
67 used as molecular markers in source apportionment models (Marmur et al., 2006; Schauer and Cass,
68 2000; Schauer et al., 1996; Robinson et al., 2006; Chow et al., 2007; Arhami et al., 2018; Esmailirad
69 et al., 2020; Tian et al., 2021a; Mancilla et al., 2021). An organic molecular marker-based chemical
70 mass balance (OM-CMB) method has been widely used to quantify source contributions to
71 carbonaceous aerosols. The OM-CMB method performs well in the source apportionment of OC, but
72 does not directly estimate contributions of inorganic secondary ions when apportioning PM_{2.5} sources
73 (Ke et al., 2008). Thus, it is advantageous to explore the influence of using both inorganic and organic
74 markers in the CMB modeling of PM_{2.5}.

75

76 Several studies have applied the OM-CMB model for source apportionment of PM in China (Zheng
77 et al., 2005; Liu et al., 2016; Guo et al., 2013; Wang et al., 2009; Wu et al., 2020; Xu et al., 2021).
78 However, the organic source profiles they used were mainly derived from measurements made in the
79 United States, which may be less representative of the local sources and current conditions of the
80 sources in China.

81

82 Therefore, this paper aims at exploring the influence of introducing inorganic markers, and the
83 sensitivity to source profiles. PM_{2.5} source apportionment was conducted by CMB modeling based
84 on organic markers (OM-CMB) and by a combination of organic and inorganic markers (IOM-CMB).
85 Commonly used markers (including OC, EC, ions, elements) and organic markers (including
86 polycyclic aromatic hydrocarbons (PAHs), n-alkanes, hopanes, levoglucosan, palmitic acid, stearic
87 acid, and cholesterol) in PM_{2.5} collected in a Chinese megacity were analysed. Source apportionment



88 of OC was conducted by the OM-CMB approach, and then the other source contributions to $PM_{2.5}$
89 were indirectly estimated. In addition, source apportionment of $PM_{2.5}$ was directly conducted by the
90 IOM-CMB method, and source contributions to $PM_{2.5}$ estimated by the OM-CMB and the IOM-CMB
91 methods were compared. In addition, the sensitivity to different source profiles for coal combustion
92 and gasoline vehicles were tested.

93

94 **2 METHODS AND MATERIALS**

95 **2.1 Sampling**

96 $PM_{2.5}$ samples were collected from a megacity in China, Chengdu ($102^{\circ}54'$ to $104^{\circ}53'$ E, $30^{\circ}05'$ to
97 $31^{\circ}26'$ N), from January to December in 2018. The city is located in Southwestern China with a
98 population of more than 14 million. As the capital of Sichuan province, Chengdu is a centre of
99 economic development and transportation in Southwestern China, with continuous development of
100 industry and changes in traffic conditions (Shi et al., 2015; Liu et al., 2015).

101

102 The sampling site is at the Environmental Protection Building (EPB, $104^{\circ}04'$ E, $30^{\circ}35'$ N), which is
103 located in a mixed residential and commercial area of the downtown city (Shi et al., 2017). There is
104 no obvious industrial emission near the building. The sampling points are located on the rooftop of
105 the EPB building, which is approximately 25 m above ground level. Daily samples were collected
106 and each sampling lasted for 22 h. The sampling was stopped during rainy days. There were 64 $PM_{2.5}$
107 samples collected during the whole year, involving spring (March, April and May), summer (June,
108 July and August), autumn (September, October and November), and winter (January, February and
109 December). The dry season (Jan. to Apr., Dec.) and wet season (Jun. to Oct.) were both well
110 represented.



111 The samples were collected using two medium-volume air samplers (TH-150, Wuhan Tianhong,
112 China) with a flow rate of 100 L/min. Polypropylene (90 mm in diameter) and quartz filters (90 mm
113 in diameter) were used to collect particulate matter. After sampling, the quartz filters were kept in
114 aluminum foil bags and stored at $-4\text{ }^{\circ}\text{C}$.

115

116 **2.2 Chemical analysis and quality assurance and quality control (QA/QC)**

117 The following source tracer components were analysed: OC, EC, ions, elements, PAHs, n-alkanes,
118 hopane, levoglucosan, fatty acids, and cholesterol. The particles collected on the polypropylene filters
119 were used for the analysis of elements including Si, Ca, Al by inductively coupled plasma-mass
120 spectrometry (ICP-AES) (IRIS Intrepid II, Thermo Electron). A 1/4 section of each filter was placed
121 into an acid solution (HNO_3 : HCl : $\text{H}_2\text{O}_2 = 1: 3: 1$). The quartz filters were used for the analysis of the
122 water-soluble ions (NH_4^+ , Cl^- , NO_3^- and SO_4^{2-}) and carbon fractions (OC and EC). A 1/8 portion of
123 each filter was cut and placed in a centrifuge tube with 8 ml of distilled deionized water and the
124 solutions were refrigerated for 24 hours, filtered and analyzed with a Thermo ICS900 Ion
125 Chromatograph (Thermo Electron) (Tian et al., 2013). Carbon components were measured by a
126 thermal/optical carbon aerosol analyzer (DRI 2001A, Atmoslytic Inc.) based on the IMPROVE
127 thermal/optical reflectance (TOR) protocol.

128

129 Organic compounds, including 11 n-alkanes, 17 PAHs, 3 hopanes, 2 fatty acids, levoglucosan and
130 cholesterol, were measured by gas chromatography-mass spectrometry (GC-MS). The full names and
131 corresponding abbreviations of the components are summarized in Table 1.

132

133 A 1/4 of each quartz filter was cut and put into a tube prior to analysis of PAHs, n-alkanes, and hopane.



134 It underwent a sonicated extraction with 20 mL dichloromethane and n-hexane (v/v 1:1) under ice
135 bath conditions twice, each for 15 min, and filtration into a round-bottomed flask by a 0.22 μm filter.
136 After passage through a pre-activated solid phase extraction cartridge and elution with n-hexane, the
137 solution was concentrated under reduced pressure on a rotary evaporator to near dryness (less than 5
138 ml). Finally, the volume was reduced to 1 ml after a slow nitrogen blow. The internal standards
139 (naphthalene-d8, acenaphthene-d10, phenanthrene-d10, chrysene-d12, and perylene-d12;
140 hexamethylbenzene; n-tetracosane-d50) were added to the samples and the samples were stored at
141 under $-4\text{ }^{\circ}\text{C}$ in darkness until analysis (Liu et al., 2015).

142

143 Another 1/4 of the quartz filters was cut and put into tubes to analyze fatty acids and cholesterol.
144 Fifteen ml methanol and 10 ml dichloromethane (v/v 1:2) were added into the tubes and sonicated,
145 then extracted for 10 min 3 times. The solution was filtered into a round-bottomed flask using a 0.22
146 μm filter. After concentration by a rotary evaporator to near 5 ml, the solution was concentrated to 1
147 ml by a high purity nitrogen gas stream. The extract was derivatized by BSTFA plus 1% TMCS at
148 $70\text{ }^{\circ}\text{C}$ for 2 h, and used for analyzing the concentrations of n-alkanoic acids and cholesterol (He et
149 al., 2006; Schauer et al., 1999). The internal standard (hexamethylbenzene) was added to the samples.
150 The last 1/4 of the quartz filters was cut and put into a tube to analyze levoglucosan through a high-
151 performance anion-exchange chromatography with pulsed amperometric detection (HPAEC-PAD)
152 (Herisau, Switzerland) with a Hamilton RCX-30 250 column.

153

154 The other organic markers were analyzed by GC-MS (7890B/5977B, Agilent, USA) using a 30m \times
155 0.25 mm diameter DB-5MS capillary column (0.25 μm film thickness). The carrier gas was pure
156 helium (purity of 99.99% or more) at a constant flow rate of 1.0 mL min^{-1} . For PAHs and hopanes,



157 inlet and transfer line temperatures were set to 230°C and 280°C respectively. For n-alkane analysis,
158 inlet and transfer line temperatures were set to 300°C. EI mode was used and the ionization energy
159 level was 70eV.

160

161 Quality assurance and control were highly valued throughout the whole experiment. All samples and
162 blank filters were analyzed using the same methods. Quartz filters were baked in an oven before use
163 to remove organic interference. Before and after sampling, all the filters were equilibrated at the same
164 environmental condition for 48 h in desiccators before weighing. Each filter was weighted by a
165 sensitive microbalance with balance sensitivity ± 0.010 mg.

166

167 Field and laboratory blanks were measured to correct the corresponding data. The same procedure
168 was used to analyze standards every day, including standards for each n-alkane, PAHs mixture, each
169 hopane (O2Si Smart Solutions, USA); standards for PALMIA, STEARA, and CHOL (Dr.
170 Ehrenstorfer, Germany); and standard for LEVOG (U.S. Pharmacopeia, USA). The recovery values
171 of all target components showed a low relative standard deviation. In addition, the first sample of
172 every ten samples was re-examined and the precision was found to be within 10%. The recoveries
173 were 79-106% for elements, and 96-110% for ions. For carbon fractions, a system stability test (three-
174 peak detection) is required before and after detecting samples and the relative standard deviation
175 should not exceed 5%. The recoveries of most organic compounds ranged from 60%-130%.

176

177 In addition, the chemical species were reconstructed using the following equations referred to in the
178 IMPROVE Report V (Hand et al., 2011):

179



180 Ammonium sulphate = $1.375[\text{SO}_4^{2-}]$ (1)

181 Ammonium nitrate = $1.29[\text{NO}_3^-]$ (2)

182 Organic matter (OM) = $1.8[\text{OC}]$ (3)

183 Crustal material = $2.2[\text{Al}] + 2.49[\text{Si}] + 1.63[\text{Ca}] + 2.42[\text{Fe}] + 1.94[\text{Ti}]$ (4)

184 Other = PM-sulphate-nitrate-organic matter-crustal material-EC (5)

185

186 **2.3 Chemical Mass Balance (CMB) Modelling**

187 The CMB model has been used extensively as a receptor model in air pollution source apportionment
188 studies. The model is mainly based on two assumptions: 1) The measured chemical and physical
189 properties must present in different proportions in different source emissions, and 2) the changes in
190 these proportions are negligible or can be approximated during the process of particulate matter
191 transport from the source to the receptor (Watson et al., 2002). Two methods were used to conduct
192 the source apportionment of $\text{PM}_{2.5}$. The organic marker-based CMB (OM-CMB) model was used in
193 this study to apportion the sources of OC and $\text{PM}_{2.5}$ (Schauer et al., 1996; Villalobos et al., 2017).
194 This model was applied to determine the primary source contributions (including gasoline vehicles,
195 diesel vehicles, industrial coal combustion, resuspended dust, biomass burning, cooking, and
196 vegetation detritus) to OC, and the contributions of the primary emission sources to $\text{PM}_{2.5}$ were
197 calculated using the ratios of $\text{PM}_{2.5}$ mass to fine OC in each source. The SO_4^{2-} and NO_3^- were not
198 included in the OM-CMB modeling, but they were measured in the profiles of above primary sources,
199 so the contributions of secondary SO_4^{2-} and NO_3^- were calculated by the difference between the
200 measured concentrations and the amount estimated in the primary source emissions (Zheng et al.,
201 2002), and then they were converted to ammonium sulphate and ammonium nitrate using the
202 equations (1) and (2) above. In addition, the secondary organic carbon (SOC) was considered as the



203 unresolved source, and was calculated as the difference between measured OC and the sum of all
204 significant contributions to OC (Villalobos et al., 2017).

205

206 For the inorganic and organic marker-based CMB (IOM-CMB) model, PM_{2.5} source apportionment
207 was conducted based on inorganic and organic source profiles as showed in Table 1. The profiles of
208 gasoline vehicles, diesel vehicles, industrial coal combustion, resuspended dust, biomass burning,
209 cooking, soil dust, sulphate, and nitrate were inputted into the CMB model, and their contributions
210 were directly obtained. The SOC was also calculated as the difference between measured OC and the
211 sum of all primary contributions to OC, and then was converted to SOA through equation (3). The
212 other difference from the OM-CMB is that the source profiles of vegetation detritus did not work in
213 this calculation, and a soil dust profile was used. Although they are two different source categories,
214 their profiles are similarly characterized by high loadings of C31 and C33 n-alkanes (Tian et al.,
215 2021b) due to vegetation influence. Details of the source profiles used in the two methods will be
216 discussed in Section 2.4. The components introduced into the OM-CMB and IOM-CMB are
217 summarized in Table 1.

218

219 To ensure the reliability of the fitting results, the following parameters were used to evaluate the
220 model outputs of the two methods. The percent mass explained by the model is typically between 80
221 and 120%. For goodness-of-fit parameters, high r^2 (>0.8) and low χ^2 (<4) were required. In addition,
222 the MPIN (modified pseudo inverse normalized) matrix was checked to determine the marker of each
223 source category.

224

225 In addition, an independent estimation of the SOA was also conducted by the EC tracer method



226 (defined as the SOA_{EC}) to compare with the SOA estimated the OM-CMB and IOM-CMB. Assuming
227 EC totally comes from primary sources and the OC/EC ratio in primary sources is relatively constant,
228 SOA_{EC} was estimated as in Turpin and Huntzicker (1995):

229

$$230 \quad SOA_{EC} = OC - EC * (OC/EC)_{pri} \quad (6)$$

$$231 \quad SOA_{EC} = 1.8 [SOA_{EC}] \quad (7)$$

232

233 where OC and EC are the measured ambient concentrations; $(OC/EC)_{pri}$ is the OC/EC ratio in primary
234 aerosols. $(OC/EC)_{pri}$ values of 2.0-2.2 are usually applied to identify and estimate SOA (Xu et al.,
235 2021). In this study, the lowest OC/EC ratio of all samples was observed as 2.0, so $(OC/EC)_{pri}=2.0$
236 was used.

237

238 **2.4 Source Profiles**

239 The source profiles applied in this study include: (1) gasoline vehicles, diesel vehicles, coal
240 combustion, resuspended dust and soil dust which were measured by ourselves (Tian et al., 2021b);
241 (2) biomass burning (Wang et al., 2009; Pirovano et al., 2010), cooking (Zhao et al., 2015), and
242 vegetative detritus (Rogge et al., 1993; Hildemann et al., 1991) from other publications; and (3)
243 ammonium sulfate and ammonium nitrate which were used to represent secondary sulphate and
244 nitrate. To test the sensitivity of CMB results to source profiles, two different profiles of coal
245 combustion (residential vs. industrial coal combustion as in Tian et al., 2021b) and seven different
246 profiles of gasoline vehicles (as in Tian et al. (2021b) vs. those from U.S. noncatalyst vehicles in
247 Schauer et al. (2002) and from Chinese gasoline vehicles in Cai et al. (2017) were evaluated for CMB
248 modelling. Inorganic ions and elements were not showed in the Cai et al. (2017), so only OM-CMB



249 can be compared.

250

251 **3. RESULTS AND DISCUSSION**

252 **3.1 PM_{2.5} Chemical Composition**

253 The daily concentrations of the PM_{2.5} and mass closure of main species are shown in Figure 1a. PM_{2.5}
254 concentrations ranged from 28 to 237 $\mu\text{g m}^{-3}$. For the mass closure of PM_{2.5} chemical composition
255 referred to the equations (1) to (5), the fractions were in the order of OM (29%) > nitrate (24%) >
256 crustal material (23%) > sulphate (15%) > EC (5%). The daily mass closures were generally
257 consistent with the daily PM_{2.5} concentrations.

258

259 The daily concentrations of organic components are shown in Figure 1b to 1e. Their concentrations
260 were in the order of $\sum_{10}\text{n-alkanes}$ (99-393 ng m^{-3}) > levoglucosan (16-894 ng m^{-3}) > $\sum_{\text{unsaturated}}$
261 fatty acids and cholesterol (29-157 ng m^{-3}) > $\sum_{14}\text{PAHs}$ (1-96 ng m^{-3}) > $\sum_3\text{hopanes}$ (1-31 ng m^{-3}).
262 The concentrations of n-alkanes, levoglucosan, PAHs and hopanes showed similar temporal
263 variations with PM_{2.5} concentrations, while unsaturated fatty acids and cholesterol showed different
264 variations.

265

266 **3.2 Source Contributions to OC**

267 The annual average of the source contributions to OC estimated by the OM-CMB is shown in Figure
268 2a. The highest contributor for OC was SOC (34%), followed by biomass burning (17%), diesel
269 vehicles (10%), industrial coal combustion (9%), gasoline vehicles (8%), resuspended dust (8%),
270 vegetation detritus (8%), and cooking (6%).

271



272 The daily percentage contributions to OC are shown in Figure 3a. The highest daily contributions to
273 OC reached $6 \mu\text{g m}^{-3}$ for gasoline vehicles, $4 \mu\text{g m}^{-3}$ for diesel vehicles, $3 \mu\text{g m}^{-3}$ for industrial coal
274 combustion, $4 \mu\text{g m}^{-3}$ for resuspended dust, $8 \mu\text{g m}^{-3}$ for biomass burning, $2 \mu\text{g m}^{-3}$ for cooking, $3 \mu\text{g}$
275 m^{-3} for vegetation detritus, and $14 \mu\text{g m}^{-3}$ for SOC. The percentage contributions of gasoline vehicles
276 were higher during January when the $\text{PM}_{2.5}$ concentrations were the highest (due to a heavy pollution
277 episode). The percentage contributions of industrial coal combustion were higher during the dry
278 season. The biomass burning showed higher fractions during autumn and winter. The high vegetation
279 detritus concentrations were mainly observed during spring (April). The higher SOA fractions were
280 observed during August to October when photochemistry is most active and primary emissions of
281 some components are lower. The contributions of diesel vehicles, resuspended dust, and cooking
282 showed no obvious seasonal variation.

283

284 **3.3 Source Contributions to $\text{PM}_{2.5}$**

285 As described in the methods section, for the OM-CMB model, the source contributions to $\text{PM}_{2.5}$ were
286 converted from the contributions to OC. The average source contributions and conversion ratios are
287 summarized in Table S1. For the IOM-CMB model, the source contributions to $\text{PM}_{2.5}$ were directly
288 estimated. Figures 2b and 2c describe the annual average source contributions to $\text{PM}_{2.5}$. The
289 percentage contributions of gasoline vehicles, diesel vehicles, industrial coal combustion,
290 resuspended dust, biomass burning, cooking, vegetation detritus, SOA, sulphate, and nitrate were 4%,
291 10%, 15%, 12%, 5%, 3%, 4%, 9%, 10%, and 20% for OM-CMB, and 4%, 11%, 15%, 17%, 6%, 2%,
292 5%, 10%, 7%, and 18% for IOM-CMB.

293

294 The daily percentage contributions to $\text{PM}_{2.5}$ estimated by the two methods are shown in Figures 3b



295 and 3c, and the absolute contributions are shown in Figure 4. The highest daily contributions to PM_{2.5}
296 reached 21 and 20 $\mu\text{g m}^{-3}$ for gasoline vehicles, 28 and 24 $\mu\text{g m}^{-3}$ for diesel vehicles, 33 and 39 $\mu\text{g m}^{-3}$
297 $\mu\text{g m}^{-3}$ for industrial coal combustion, 34 and 34 $\mu\text{g m}^{-3}$ for resuspended dust, 17 and 17 $\mu\text{g m}^{-3}$ for biomass
298 burning, 6 and 6 $\mu\text{g m}^{-3}$ for cooking, 8 and 8 $\mu\text{g m}^{-3}$ for vegetation detritus, 26 and 25 $\mu\text{g m}^{-3}$ for SOA,
299 28 and 21 $\mu\text{g m}^{-3}$ for sulphate, and 75 and 66 $\mu\text{g m}^{-3}$ for nitrate, estimated by the OM-CMB and IOM-
300 CMB models, respectively.

301

302 As shown in Figure 3b, 3c and 4, the temporal variations of source contributions to PM_{2.5} were similar
303 to those to OC. The gasoline vehicles showed obvious higher contributions during the cold period.
304 Studies have shown that gasoline vehicles emit more PM under poor combustion conditions, such as
305 cold starts at low temperature (Schauer et al., 1999 and 2003). The percentage contributions of
306 industrial coal combustion were higher during the dry season. Hydropower supplies a large
307 percentage of Chengdu's electricity demand during the wet season, while coal combustion is needed
308 for electricity generation during the dry season (Shi et al., 2016). Biomass burning showed higher
309 fractions during autumn and winter, due to residential use and local straw burning activities. A high
310 vegetation detritus/soil dust contribution was mainly observed during spring, while the resuspended
311 dust showed weaker seasonal variations. The vegetation detritus and soil dust are natural sources, and
312 their contributions are associated respectively with vegetation and meteorological condition. The
313 resuspended dust can be caused by high wind strength and intensive human activities (such as road
314 dust caused by heavy traffic, construction dust caused by building activities, etc.).

315

316 The highest percentage contributions of SOA and sulphate were observed during August to October.
317 Their formation is associated with photochemical processes which are more efficient because of



318 strong illumination, less precipitation and high temperature during August to October. The SOA and
319 sulphate also showed higher contributions during January. Although photochemical reactions may be
320 generally weak during January, high precursor concentrations, humidity and PM during winter may
321 enhance the aqueous phase and heterogeneous reactions. The highest fraction of nitrate occurred
322 when the temperature was low (as shown in Figure 1). Although photochemical reactions are
323 favourable in summer, nitrate may decompose at higher temperatures due to the thermodynamic
324 instability of ammonium nitrate (Hasheminassab et al., 2014), and the high relative humidity during
325 wintertime in Chengdu can enhance the secondary formation of nitrate through heterogeneous
326 reactions (Liu et al., 2019).

327

328 **3.4 Comparisons of Daily Source Contributions and markers**

329 In this study, except for the soil dust and vegetation detritus, similar source categories were shared by
330 the OM-CMB and IOM-CMB. Thus, a comparison of the contributions estimated by the two CMB
331 methods was conducted. Furthermore, the contributions were also compared with the corresponding
332 markers which had high MPIN values. The temporal variations of source contributions and
333 corresponding markers which had high MPIN were compared, as shown in Figure 4.

334

335 It can be seen that the average contributions of sulphate and nitrate from the OM-CMB were higher
336 than those from the IOM-CMB (as shown in Figure 2), while their daily contributions were highly
337 consistent with each other and with the trends of corresponding markers. The sulfate and nitrate
338 sources from the OM-CMB are the measured values after subtracting the summed mass of sulfate and
339 nitrate emitted from the selected primary sources as described in the section 2.3, while those from the
340 IOM-CMB were directly estimated by the CMB model. The consistent temporal variations of



341 contributions indicate they were well estimated by the two methods due to the low collinearity. The
342 difference of average contributions might be caused by uncertainties in the estimation of primary
343 source contributions (such as in resuspended dust), if the actual source compositions differs from the
344 profiles used in the model. As shown in Figure 4, the average values and temporal variations of the
345 SOA from two methods were also in agreement with each other, and with the SOA_{EC} which was
346 independently estimated by the EC tracer method according to equations (6) to (7). The SOA
347 estimated by the IOM-CMB was more consistent with the SOA_{min} than that estimated by the OM-
348 CMB, because EC was used in the IOM-CMB.

349

350 According to Figure 2, among the primary source categories, the average contributions of the gasoline
351 vehicles, diesel vehicles, industrial coal combustion and cooking estimated by the two methods were
352 generally consistent, and the average contributions of resuspended dust and dust/vegetation detritus
353 showed larger differences for the two methods. What's more, as shown in Figure 4, the daily
354 variability of biomass burning and gasoline vehicles from two methods showed more consistent
355 temporal variations (with squared correlation coefficient $R^2=0.87$ and 0.86) than other primary
356 sources (with R^2 ranged from 0.53 to 0.67). The biomass burning and gasoline vehicle contributions
357 also showed similar temporal variations with their corresponding markers. The marker of gasoline
358 vehicles was BghiP and the marker of biomass burning was LEVOG, which were very different from
359 other sources, so their low collinearity with other sources can explain the consistent results. The daily
360 contributions of diesel vehicles and industrial coal combustion of the two methods were moderately
361 consistent. Consistent markers were identified for these two sources by the OM-CMB and IOM-CMB;
362 however, the collinearity between source profiles of diesel vehicles and industrial coal combustion
363 may cause some differences. For example, they are both characterized by high loadings of C24, C25



364 alkanes and medium-ring PAHs (Tian et al., 2021b). The contributions of resuspended dust estimated
365 by the two methods showed differences, probably because different markers (C31 for OM-CMB and
366 Ca for IOM-CMB) were identified for CMB modeling. Cooking contributions estimated by the two
367 methods also showed weak correlations with each other and with the corresponding marker, which
368 may be due to its contributions being generally low and influenced by other source categories. The
369 STEARA also exists in the source profiles of other sources, so the differences of other source
370 contributions can influence its attribution and the cooking contribution.

371

372 **3.5 Sensitivity of Source Apportionment to Source Profiles**

373 Two different profiles for two major sources - coal combustion and gasoline vehicles - were used to
374 test the sensitivity to source profiles as mentioned above. The result of the IOM-CMB which used the
375 residential coal combustion instead of industrial coal combustion profile is shown in Figure S1.
376 Compared with the result for the industrial coal combustion, the contributions of resuspended dust
377 and residential coal combustion were higher, and the contributions of other sources were lower. The
378 difference between two coal combustion profiles was that the residential coal combustion showed
379 higher OC and organic compounds and lower crustal elements than the industrial coal combustion
380 (Tian et al., 2021b). The lower crustal elements in the residential coal combustion may explain the
381 overestimation of the resuspended dust, whose markers were mainly crustal elements, when using its
382 profile. Residential coal combustion is an important source category in northern China, but there is
383 little in the central city of southern China. Thus, the industrial coal combustion source profile was
384 selected in this study.

385

386 For the gasoline vehicle profiles, most results did not meet the goodness-of-fit criteria when using the



387 noncatalyst vehicle profile measured by Schauer et al. (2002). Figure S2 describes the OC-CMB
388 results using the Chinese gasoline vehicle profiles measured by Cai et al. (2017). Except for the heavy
389 gasoline 2, most results were comparable with the results using our gasoline vehicle profiles. In
390 summary, it is important to use local and up-to-date source profiles for the source apportionment, and
391 to include more components in the profiles.

392

393 **4 CONCLUSIONS**

394 To explore the influence of introducing inorganic markers and sensitivity to source profiles, a
395 comprehensive comparison of PM_{2.5} source apportionment using organic marker-based OM-CMB as
396 well as organic and inorganic marker-based IOM-CMB was conducted. The percentage contributions
397 of gasoline vehicles, diesel vehicles, industrial coal combustion, resuspended dust, biomass burning,
398 cooking, vegetation detritus, SOA, sulphate, and nitrate were 4%, 10%, 15%, 12%, 5%, 3%, 4%, 9%,
399 10%, and 20% for OM-CMB, and 4%, 11%, 15%, 17%, 6%, 2%, 5%, 10%, 7%, and 18% for IOM-
400 CMB. The temporal variations of PM_{2.5} contributions from sulphate, nitrate, SOA, gasoline vehicles,
401 and biomass burning were in good agreement between the OM-CMB and IOM-CMB results. The
402 OM-CMB and IOM-CMB are powerful to apportion sources characterized by unique markers (such
403 as biomass combustion) and low collinearity. The diesel vehicle and industrial coal combustion
404 estimates were moderately consistent between the two methods. The OM-CMB resuspended dust and
405 cooking estimates showed poor correlation with the IOM-CMB results. The discrepancy in
406 resuspended dust between OM-CMB and IOM-CMB may be due to the different tracers in their
407 source profiles. In addition, when testing the sensitivity to source profiles for two coal combustion
408 and two gasoline vehicle profiles, it was found important to use current and relevant source profiles
409 according to local source information for the source apportionment.



410 **DATA ACCESSIBILITY**

411 Data supporting this publication are openly available from the UBIRA eData repository at
412 (<https://doi.org/10.25500/edata.bham.00000745>)

413

414 **AUTHOR CONTRIBUTIONS**

415 YZ and RMH conceived the study. YZ, RMH, and ZS guided the work and wrote the paper. XW and
416 PZ carried out the chemical analysis and data analysis.

417

418 **COMPETING INTERESTS**

419 The authors declare that they have no conflict of interest.

420

421 **FINANCIAL SUPPORT**

422 This research has been supported by the National Natural Science Foundation of China (41977181),
423 and Young Elite Scientists Sponsorship Program by Tianjin, China (TJSQNTJ-2018-04). RMH and
424 ZS are supported by Natural Environment Research Council (NE/N007190/1).

425

426



427 **REFERENCE**

428

429 Arhami, M., Shahne, M. Z., Hosseini, V., Haghghat, N. R., Lai, A. M., and Schauer, J. J.: Seasonal
430 trends in the composition and sources of PM_{2.5} and carbonaceous aerosol in Tehran, Iran, *Environ.*
431 *Pollut.*, 239, 69-81, <https://doi.org/10.1016/j.envpol.2018.03.111>, 2018.

432

433 Bell, M. L., Ebisu, K., Leaderer, B. P., Gent, J. F., Lee, H. J., Koutrakis, P., Wang, Y., and Dominici,
434 F., Peng, R. D.: Associations of PM_{2.5} constituents and sources with hospital admissions: Analysis
435 of four counties in Connecticut and Massachusetts (USA) for persons \geq 65 years of age, *Environ.*
436 *Health. Perspect.*, 122, 138-144, <https://doi.org/10.1289/ehp.1306656>, 2014.

437

438 Cai, T., Zhang, Y., Fang, D., Shang, J., Zhang, Y., and Zhang, Y.: Chinese vehicle emissions
439 characteristic testing with small sample size: Results and comparison, *Atmos. Pollut. Res.*, 8, 154-
440 163, <https://doi.org/10.1016/j.apr.2016.08.007>, 2017.

441

442 Cao, F., Zhang, Y. X., Lin, X., and Zhang, Y. L.: Characteristics and source apportionment of non-
443 polar organic compounds in PM_{2.5} from the three megacities in Yangtze River Delta region, China,
444 *Atmos. Res.*, 252, 105443, <https://doi.org/10.1016/j.atmosres.2020.105443>, 2021.

445

446 Chen, P. L., Wang, T. J., Hu, X., and Xie, M.: Chemical mass balance source apportionment of size-
447 fractionated particulate matter in Nanjing, China, *Aerosol Air Qual. Res.*, 15, 1855-1867,
448 <https://doi.org/10.4209/aaqr.2015.03.0172>, 2015.

449

450 Chow, J. C., Watson, J. G., Lowenthal, D. H., Chen, L. W. A., Zielinska, B., Mazzoleni, L. R., and
451 Magliano, K. L.: Evaluation of organic markers for chemical mass balance source apportionment at
452 the Fresno Supersite, *Atmos. Chem. Phys.*, 7, 1741-1754, <https://doi.org/10.5194/acp-7-1741-2007>,
453 2007.

454

455 Clappier, A., Pisoni, E., and Thunis, P.: A new approach to design source-receptor relationships for
456 air quality modelling, *Environ. Model. Softw.*, 74, 66-74,
457 <https://doi.org/10.1016/j.envsoft.2015.09.007>, 2015.

458

459 Esmailirad, S., Lai, A., Abbaszade, G., Schnelle-Kreis, J., Zimmermann, R., Uzu, G., Daellenbach,
460 K., Canonaco, F., Hassankhany, H., Arhami, M., Baltensperger, U., Prevot, A. S. H., Schauer, J. J.,
461 Jaffrezo, J. L., Hosseini, V., and El Haddad, I.: Source apportionment of fine particulate matter in a
462 Middle Eastern Metropolis, Tehran-Iran, using PMF with organic and inorganic markers, *Sci. Tot.*
463 *Environ.*, 705, 135330, <https://doi.org/10.1016/j.scitotenv.2019.135330>, 2020.

464

465 Guan, P., Wang, X., Cheng, S., and Zhang, H.: Temporal and spatial characteristics of PM_{2.5}
466 transport fluxes of typical inland and coastal cities in China, *J. Environ. Sci.*, 103, 229-245,
467 <https://doi.org/10.1016/j.jes.2020.10.017>, 2021.

468

469 Guo, S., Hu, M., Guo, Q., Zhang, X., Schauer, J. J., and Zhang, R.: Quantitative evaluation of
470 emission controls on primary and secondary organic aerosol sources during Beijing 2008 Olympics,
471 *Atmos. Chem. Phys.*, 13, 8303-8314, <https://doi.org/10.5194/acp-13-8303-2013>, 2013.



- 472 Hand, J., Copeland, S., McDade, C., Day, D., Moore Jr., C., Dillner, A., Pitchford, M., Indresand,
473 H., Schichtel, B., Malm, W., Watson, J.: Interagency monitoring of protected visual environments
474 (IMPROVE). In: *Spatial and Seasonal Patterns and Temporal Variability of Haze and its*
475 *Constituents in the United States*. Report V ISSN: 0737-5352-87, 2011.
476
- 477 Hasheminassab, S., Daher, N., Saffari, A., Wang, D., Ostro, B.D., and Sioutas, C.: Spatial and
478 temporal variability of sources of ambient fine particulate matter (PM_{2.5}) in California, *Atmos.*
479 *Chem. Phys.*, 14, 12085-12097, <https://doi.org/10.5194/acp-14-12085-2014>, 2014.
480
- 481 He, L. Y., Hu, M., Huang, X. F., Zhang, Y. H., and Tang, X. Y.: Seasonal pollution characteristics of
482 organic compounds in atmospheric fine particles in Beijing, *Sci. Tot. Environ.*, 359, 167-176,
483 <https://doi.org/10.1016/j.scitotenv.2005.05.044>, 2006.
484
- 485 Hildemann, L. M., Markowski, G. R., and Cass, G. R.: Chemical composition of emissions from
486 urban sources of fine organic aerosol, *Environ. Sci. Technol.*, 25, 744-759,
487 <https://doi.org/10.1021/es00016a021>, 1991.
488
- 489 Hong, Y., Xu, X., Liao, D., Ji, X., Hong, Z., Chen, Y., Xu, L., Li, M., Wang, H., Zhang, H., Xiao,
490 H., Choi, S.-D., and Chen, J.: Air pollution increases human health risks of PM_{2.5}-bound PAHs and
491 nitro-PAHs in the Yangtze River Delta, China, *Sci. Tot. Environ.*, 770, 145402,
492 <https://doi.org/10.1016/j.scitotenv.2021.145402>, 2021.
493
- 494 Ke, L., Liu, W., Wang, Y., Russell, A. G., Edgerton, E. S., and Zheng, M.: Comparison of PM_{2.5}
495 source apportionment using positive matrix factorization and molecular marker-based chemical
496 mass balance, *Sci. Tot. Environ.*, 394, 290-302, <https://doi.org/10.1016/j.scitotenv.2008.01.030>,
497 2008.
498
- 499 Li, X., Yan, C., Wang, C., Ma, J., Li, W., Liu, J., and Liu, Y.: PM_{2.5}-bound elements in Hebei
500 Province, China: Pollution levels, source apportionment and health risks, *Sci. Tot. Environ.*, 806,
501 150440, <https://doi.org/10.1016/j.scitotenv.2021.150440>, 2022.
502
- 503 Li, F. X., Gu, J. W., Xin, J. Y., Schnelle-Kreis, J., Wang, Y. S., Liu, Z. R., Shen, R. R., Michalke, B.,
504 Abbaszade, G., and Zimmermann, R.: Characteristics of chemical profile, sources and PAH toxicity of
505 PM_{2.5} in Beijing in autumn-winter transit season with regard to domestic heating, pollution control
506 measures and meteorology, *Chemosphere*, 276, 130143,
507 <https://doi.org/10.1016/j.chemosphere.2021.130143>, 2021.
508
- 509 Li, L., Li, Q., Huang, L., Wang, Q., Zhu, A. S., Xu, J., Liu, Z. Y., Li, H. L., Shi, L. S., Li, R., Azari,
510 M., Wang, Y. J., Zhang, X. J., Liu, Z. Q., Zhu, Y. H., Zhang, K., Xue, S. H., Ooi, M. C. G., Zhang,
511 D. P., and Chan, A.: Air quality changes during the COVID-19 lockdown over the Yangtze River
512 Delta Region: An insight into the impact of human activity pattern changes on air pollution
513 variation, *Sci. Tot. Environ.*, 732, 139282, <https://doi.org/10.1016/j.scitotenv.2020.139282>, 2020a.
514
- 515 Li, J. J., Li, J., Wang, G. H., Zhang, T., Dai, W. T., Ho, K. F., Wang, Q. Y., Shao, Y., Wu, C., and Li,
516 L.: Molecular characteristics of organic compositions in fresh and aged biomass burning aerosols,



- 517 Sci. Tot. Environ., 741, 140247, <https://doi.org/10.1016/j.scitotenv.2020.140247>, 2020b.
518
- 519 Li, R., Wang, Q. Q., He, X., Zhu, S. H., Zhang, K., Duan, Y. S., Fu, Q. Y., Qiao, L. P., Wang, Y. J.,
520 Huang, L., Li, L., and Yu, J. Z.: Source apportionment of PM_{2.5} in Shanghai based on hourly
521 organic molecular markers and other source tracers, *Atmos. Chem. Phys.*, 20, 12047-12061,
522 <https://doi.org/10.5194/acp-20-12047-2020>, 2020c.
523
- 524 Liu, F., Tan, Q., Jiang, X., Yang, F., and Jiang, W.: Effects of relative humidity and PM_{2.5} chemical
525 compositions on visibility impairment in Chengdu, China, *J. Environ. Sci.*, 86, 15-23,
526 <https://doi.org/10.1016/j.jes.2019.05.004>, 2019.
527
- 528 Liu, Q. Y., Baumgartner, J., Zhang, Y., and Schauer, J. J.: Source apportionment of Beijing air
529 pollution during a severe winter haze event and associated pro-inflammatory responses in lung
530 epithelial cells, *Atmos. Environ.*, 126, 28-35, <https://doi.org/10.1016/j.atmosenv.2015.11.031>, 2016.
531
- 532 Lu, Z. J., Liu, Q. Y., Xiong, Y., Huang, F., Zhou, J. B., and Schauer, J. J.: A hybrid source
533 apportionment strategy using positive matrix factorization (PMF) and molecular marker chemical
534 mass balance (MM-CMB) model, *Environ. Pollut.*, 238, 39-51,
535 <https://doi.org/10.1016/j.envpol.2018.02.091>, 2018.
536
- 537 Mancilla, Y., Medina, G., Gonzalez, L. T., Herckes, P., Fraser, M. P., and Mendoza, A.:
538 Determination and similarity analysis of PM_{2.5} emission source profiles based on organic markers
539 for Monterrey, Mexico, *Atmosphere*, 12, 554, <https://doi.org/10.3390/atmos12050554>, 2021.
540
- 541 Marmur, A., Park, S. K., Mulholland, J. A., Tolbert, P. E., and Russell, A. G.: Source apportionment
542 of PM_{2.5} in the southeastern United States using receptor and emissions-based models: Conceptual
543 differences and implications for time-series health studies, *Atmos. Environ.*, 40, 2533-2551,
544 <https://doi.org/10.1016/j.atmosenv.2005.12.019>, 2006.
545
- 546 Mor, S., Kumar, S., Singh, T., Dogra, S., Pandey, V., and Ravindra, K.: Impact of COVID-19 lockdown
547 on air quality in Chandigarh, India: Understanding the emission sources during controlled
548 anthropogenic activities, *Chemosphere*, 263, 127978,
549 <https://doi.org/10.1016/j.chemosphere.2020.127978>, 2021.
550
- 551 Olson, D. A., Turlington, J., Duvall, R. V., Viedow, S. R., Stevens, C. D., and Williams, R.: Indoor
552 and outdoor concentrations of organic and inorganic molecular markers: Source apportionment of
553 PM_{2.5} using low-volume samples, *Atmos. Environ.*, 42, 1742-1751,
554 <https://doi.org/10.1016/j.atmosenv.2007.11.035>, 2008.
555
- 556 Perrone, M. G., Larsen, B. R., Ferrero, L., Sangiorgi, G., De Gennaro, G., Udisti, R., Zangrando, R.,
557 Gambaro, A., and Bolzacchini, E.: Sources of high PM_{2.5} concentrations in Milan, Northern Italy:
558 Molecular marker data and CMB modelling, *Sci. Tot. Environ.*, 414, 343-355,
559 <https://doi.org/10.1016/j.scitotenv.2011.11.026>, 2012.
560
561



- 562 Pirovano, G., Colombi, C., Balzarini, A., Riva, G. M., Gianelle, V., and Lonati, G.: PM_{2.5} source
563 apportionment in Lombardy (Italy): Comparison of receptor and chemistry-transport modelling
564 results, *Atmos. Environ.*, 106, 56-70, <https://doi.org/10.1016/j.atmosenv.2015.01.073>, 2015.
- 565
- 566 Robinson, A. L., Subramanian, R., Donahue, N. M., Bernardo-Bricker, A., and Rogge, W. F.: Source
567 apportionment of molecular markers and organic aerosol. 3. Food cooking emissions, *Environ. Sci.
568 Technol.*, 40, 7820-7827, <https://doi.org/10.1021/es060781p>, 2006.
- 569
- 570 Rogge, W. F., Hildemann, L. M., Mazurek, M. A., Cass, G. R., and Simoneit, B.: Sources of fine
571 organic aerosol. 4. Particulate abrasion products from leaf surfaces of urban plants, *Environ. Sci.
572 Technol.*, 27, 2700-2711, <https://doi.org/10.1021/es00049a008>, 1993.
- 573
- 574 Schauer, J. J.: Evaluation of elemental carbon as a marker for diesel particulate matter, *J. Expo.
575 Anal. Env. Epidemiol.*, 13, 443-453, <https://doi.org/10.1038/sj.jea.7500298>, 2003.
- 576
- 577 Schauer, J. J., Kleeman, M. J., Cass, G. R., and Simoneit, B. R. T.: Measurement of emissions from
578 air pollution sources. 5. C-1-C-32 organic compounds from gasoline-powered motor vehicles,
579 *Environ. Sci. Technol.*, 36, 1169-1180, <https://doi.org/10.1021/es0108077>, 2002.
- 580
- 581 Schauer, J. J., and Cass, G. R.: Source apportionment of wintertime gas-phase and particle-phase air
582 pollutants using organic compounds as tracers, *Environ. Sci. Technol.*, 34, 1821-1832,
583 <https://doi.org/10.1021/es981312t>, 2000.
- 584
- 585 Schauer, J. J., Kleeman, M. J., Cass, G. R., and Simoneit, B. R. T.: Measurement of emissions from
586 air pollution sources. 1. C-1 through C-29 organic compounds from meat charbroiling, *Environ. Sci.
587 Technol.*, 33, 1566-1577, <https://doi.org/10.1021/es980076j>, 1999.
- 588
- 589 Schauer, J. J., Rogge, W.F., Hildemann, L. M., Mazurek, M. A., and Cass, G. R.: Source
590 apportionment of airborne particulate matter using organic compounds as tracers, *Atmos. Environ.*,
591 30, 3837-3855, [https://doi.org/10.1016/1352-2310\(96\)00085-4](https://doi.org/10.1016/1352-2310(96)00085-4), 1996.
- 592
- 593 Shi, G. L., Peng, X., Liu, J. Y., Tian, Y. Z., Song, D. L., Yu, H. F., Feng, Y. C., and Russell, A. G.:
594 Quantification of long-term primary and secondary source contributions to carbonaceous aerosols,
595 *Environ. Pollut.*, 219, 897-905, <https://doi.org/10.1016/j.envpol.2016.09.009>, 2016.
- 596
- 597 Song, L., Dai, Q., Feng, Y., and Hopke, P. K.: Estimating uncertainties of source contributions to
598 PM_{2.5} using moving window evolving dispersion normalized PMF, *Environ. Pollut.*, 286, 117576,
599 <https://doi.org/10.1016/j.envpol.2021.117576>, 2021.
- 600
- 601 Tian, Y. Z., Harrison, R. M., Feng, Y. C., Shi, Z. B., Liang, Y. L., Li, Y. X., Xue, Q. Q., and Xu, J.
602 S.: Size-resolved source apportionment of particulate matter from a megacity in northern China
603 based on one-year measurement of inorganic and organic components, *Environ. Pollut.*, 289,
604 117932, <https://doi.org/10.1016/j.envpol.2021.117932>, 2021a.
- 605
- 606 Tian, Y. Z., Liu, X., Huo, R. Q., Shi, Z. B., Sun, Y. M., Feng, Y. C., and Harrison, R. M.: Organic



- 607 compound source profiles of PM_{2.5} from traffic emissions, coal combustion, industrial processes
608 and dust, *Chemosphere*, 278, 130429, <https://doi.org/10.1016/j.chemosphere.2021.130429>, 2021b.
- 609
- 610 Tian, Y. Z., Shi, G. L., Han, S. Q., Zhang, Y. F., Feng, Y. C., Liu, G. R., Gao, L. J., Wu, J. H., and
611 Zhu, T.: Vertical characteristics of levels and potential sources of water-soluble ions in PM₁₀ in a
612 Chinese megacity, *Sci. Tot. Environ.*, 447, 1-9, <https://doi.org/10.1016/j.scitotenv.2012.12.071>,
613 2013.
- 614
- 615 Turpin, B. J., and Huntzicker, J. J.: Identification of secondary organic aerosol episodes and
616 quantitation of primary and secondary organic aerosol concentrations during SCAQS, *Atmos.*
617 *Environ.*, 29, 3527-3544, [https://doi.org/10.1016/1352-2310\(94\)00276-Q](https://doi.org/10.1016/1352-2310(94)00276-Q), 1995.
- 618
- 619 Villalobos, A. M., Barraza, F., Jorquera, H., and Schauer, J. J.: Wood burning pollution in southern
620 Chile: PM_{2.5} source apportionment using CMB and molecular markers, *Environ. Pollut.*, 225, 514-
621 523, <https://doi.org/10.1016/j.envpol.2017.02.069>, 2017.
- 622
- 623 Wang, J., Hu, Z. M., Chen, Y. Y., Chen, Z. L., and Xu, S. Y.: Contamination characteristics and
624 possible sources of PM₁₀ and PM_{2.5} in different functional areas of Shanghai, China, *Atmos.*
625 *Environ.*, 68, 221-229, <https://doi.org/10.1016/j.atmosenv.2012.10.070>, 2013.
- 626
- 627 Wang, Q., Shao, M., Zhang, Y., Wei, Y., Hu, M., and Guo, S.: Source apportionment of fine organic
628 aerosols in Beijing, *Atmos. Chem. Phys.*, 9, 9043-9080, <https://doi.org/10.5194/acp-9-8573-2009>,
629 2009.
- 630
- 631 Watson, J. G., Zhu, T., Chow, J. C., Engelbrecht, J., Fujita, E. M., and Wilson, W. E.: Receptor
632 modeling application framework for particle source apportionment, *Chemosphere*, 49, 1093-1136,
633 [https://doi.org/10.1016/S0045-6535\(02\)00243-6](https://doi.org/10.1016/S0045-6535(02)00243-6), 2002.
- 634
- 635 Wen, J., Chuai, X., Gao, R., and Pang, B.: Regional interaction of lung cancer incidence influenced
636 by PM_{2.5} in China, *Sci. Tot. Environ.*, 803, 149979,
637 <https://doi.org/10.1016/j.scitotenv.2021.149979>, 2022.
- 638
- 639 Wong, Y. K., Huang, X. H. H., Cheng, Y. Y., and Yu, J. Z.: Estimating primary vehicular emission
640 contributions to PM_{2.5} using the Chemical Mass Balance model: Accounting for gas-particle
641 partitioning of organic aerosols and oxidation degradation of hopanes, *Environ. Pollut.*, 291,
642 118131, <https://doi.org/10.1016/j.envpol.2021.118131>, 2021.
- 643
- 644 Wu, X. F., Chen, C. R., Vu, T. V., Liu, D., Baldo, C., Shen, X. B., Zhang, Q., Cen, K., Zheng, M.,
645 He, K. B., Shi, Z. B., and Harrison, R. M.: Source apportionment of fine organic carbon (OC) using
646 receptor modelling at a rural site of Beijing: Insight into seasonal and diurnal variation of source
647 contributions, *Environ. Pollut.*, 266, 115078, <https://doi.org/10.1016/j.envpol.2020.115078>, 2020.
- 648
- 649 Xu, J. S., Liu, D., Wu, X. F., Vu, T., Zhang, Y. L., Fu, P. Q., Sun, Y. L., Xu, W. Q., Zheng, B.,
650 Harrison, R. M., and Shi, Z. B.: Source apportionment of fine organic carbon at an urban site of
651 Beijing using a chemical mass balance model, *Atmos. Chem. Phys.*, 21, 7321-7341,



- 652 <https://doi.org/10.5194/acp-21-7321-2021>, 2021.
- 653
- 654 Yang, Y., Ruan, Z., Wang, X., Yang, Y., Mason, T. G., Lin, H., and Tian, L.: Short-term and long-
655 term exposures to fine particulate matter constituents and health: A systematic review and meta-
656 analysis, *Environ. Pollut.*, 247, 874-882, <https://doi.org/10.1016/j.envpol.2018.12.060>, 2019.
- 657
- 658 Yin, J., Cumberland, S. A., Harrison, R. M., Allan, J., Young, D. E., Williams, P. I., and Coe, H.:
659 Receptor modelling of fine particles in southern England using CMB including comparison with
660 AMS-PMF factors, *Atmos. Chem. Phys.*, 15, 2139-2158, doi:10.5194/acp-15-2139-2015, 2015.
- 661
- 662 Zhan, J. L., Feng, Z. M., Liu, P. F., He, X. W., He, Z. M., Chen, T. Z., Wang, Y. F., He, H., Mu, Y. J.,
663 and Liu, Y. C.: Ozone and SOA formation potential based on photochemical loss of VOCs during
664 the Beijing summer, *Environ. Pollut.*, 285, 117444, <https://doi.org/10.1016/j.envpol.2021.117444>,
665 2021.
- 666
- 667 Zhang, C., Jing, D., Wu, C., Li, S., Cheng, N., Li, W., Wang, G., Chen, B., Wang, Q., and Hu, J.:
668 Integrating chemical mass balance and the community multiscale air quality models for source
669 identification and apportionment of PM_{2.5}, *Process. Saf. Environ.*, 149, 665-675,
670 <https://doi.org/10.1016/j.psep.2021.03.033>, 2021a.
- 671
- 672 Zhang, D., He, B., Yuan, M. H., Yu, S. J., Yin, S. S., and Zhang, R. Q.: Characteristics, sources and
673 health risks assessment of VOCs in Zhengzhou, China during haze pollution season, *J. Environ.*
674 *Sci.*, 108, 44-57, <https://doi.org/10.1016/j.jes.2021.01.035>, 2021b.
- 675
- 676 Zhang, Y. L., Zhu, B., Gao, J. H., Kang, H. Q., Yang, P., Wang, L. L., and Zhang, J. K.: The source
677 apportionment of primary PM_{2.5} in an aerosol pollution event over Beijing-Tianjin-Hebei region
678 using WRF-Chem, China, *Aerosol Air Qual. Res.*, 17, 2966-2980,
679 <https://doi.org/10.4209/aaqr.2016.10.0442>, 2017.
- 680
- 681 Zhang, R., Jing, J., Tao, J., Hsu, S. C., Wang, G., Cao, J., Lee, C. S. L., Zhu, L., Chen, Z., Zhao, Y.,
682 and Shen, Z.: Chemical characterization and source apportionment of PM_{2.5} in Beijing: Seasonal
683 perspective, *Atmos. Chem. Phys.*, 13, 7053-7074, <https://doi.org/10.5194/acp-13-7053-2013>, 2013.
- 684
- 685 Zhao, X. Y., Hu, Q. H., Wang, X. M., Ding, X., He, Q. F., Zhang, Z., Shen, R. Q., Lu, S. J., Liu, T.
686 Y., Fu, X. X., and Chen, L. G.: Composition profiles of organic aerosols from Chinese residential
687 cooking: case study in urban Guangzhou, south China, *J. Atmos. Chem.*, 72, 1-18,
688 <https://doi.org/10.1007/s10874-015-9298-0>, 2015.
- 689
- 690 Zhao, P. S., Dong, F., He, D., Zhao, X. J., Zhang, X. L., Zhang, W. Z., Yao, Q., and Liu, H. Y.:
691 Characteristics of concentrations and chemical compositions for PM_{2.5} in the region of Beijing,
692 Tianjin, and Hebei, China, *Atmos. Chem. Phys.*, 13, 4631-4644, <https://doi.org/10.5194/acp-13-4631-2013>, 2013.
- 693
- 694
- 695 Zheng, M., Salmon, L. G., Schauer, J. J., Zeng, L. M., Kiang, C. S., Zhang, Y. H., and Cass, G. R.:
696 Seasonal trends in PM_{2.5} source contributions in Beijing, China, *Atmos. Environ.*, 39, 3967-3976,



697 <https://doi.org/10.1016/j.atmosenv.2005.03.036>, 2005.
698
699 Zheng, M., Cass, G. R., Schauer, J. J., and Edgerton, E. S.: Source apportionment of PM_{2.5} in the
700 Southeastern United States using solvent-extractable organic compounds as tracers, Environ. Sci.
701 Technol., 36, 2361, <https://doi.org/10.1021/es011275x>, 2002.
702
703



704 **TABLE CAPTION**

705

706 **Table 1:** Full names and abbreviations of the components used in the OM-CMB and
707 IOM-CMB.

708

709

710 **FIGURE CAPTIONS**

711

712 **Figure 1:** The daily concentrations of $PM_{2.5}$, mass closure of main species, and organic
713 components. (a) Mass closure of main species; (b) n-alkanes; (c) PAHs; (d) hopanes;
714 (e) unsaturated fatty acids and cholesterol.

715

716 **Figure 2:** (a) The average of percentage contributions to OC estimated by the OM-CMB; (b) The
717 annual average of percentage contributions to $PM_{2.5}$ estimated by the OM-CMB; (c)
718 The annual average of percentage contributions to $PM_{2.5}$ estimated by the IOM-CMB;
719 (d) Comparison of contributions to $PM_{2.5}$ estimated by the OM-CMB and IOM-CMB.

720

721 **Figure 3:** (a) Daily contributions to OC estimated by the OM-CMB; (b) Daily contributions to
722 $PM_{2.5}$ estimated by the OM-CMB; (c) Daily contributions to $PM_{2.5}$ estimated by the
723 IOM-CMB.

724

725 **Figure 4:** Comparisons among source contributions estimated by the OM-CMB and IOM-CMB,
726 and corresponding markers.

727

728



729 **Table 1.** Full names and abbreviations of the components used in the OM-CMB and IOM-CMB.
 730

Components	Abbreviations	Used in OM-CMB	Used in IOM-CMB
organic carbon	OC		Yes
element carbon	EC		Yes
ammonium	NH ₄ ⁺		Yes
chloride	Cl ⁻		Yes
nitrate	NO ₃ ⁻		Yes
sulfate	SO ₄ ²⁻		Yes
aluminum	Al		Yes
silicon	Si		Yes
calcium	Ca		Yes
polycyclic aromatic hydrocarbons	PAHs		
phenanthrene	Phe	Yes	Yes
anthracene	Ant	Yes	Yes
fluoranthene	Flt	Yes	Yes
pyrene	Pyr	Yes	Yes
benz(a)anthracene	BaA	Yes	Yes
chrysene	Chr	Yes	Yes
benzo(b)fluoranthene	BbF	Yes	Yes
benzo(k)fluoranthene	BkF	Yes	Yes
benzo(e)pyrene	BeP	Yes	Yes
benzo(a)pyrene	BaP	Yes	Yes
dibenz(a,h)anthracene	DBA	Yes	Yes
Indeno(1,2,3-cd)pyrene	IPY	Yes	Yes
benzo(ghi)perylene	BghiP	Yes	Yes
coronene	Cor	Yes	Yes
hopanes			
17 α (H)-22,29,30-Trisnorhopane	C27a	Yes	Yes
17 α (H),21 β (H)-30-Norhopane	C29ab	Yes	Yes
17 α (H),21 β (H)-hopane	C30ab	Yes	Yes
n-alkanes			
n-tetracosane	C24	Yes	Yes
n-pentacosane	C25	Yes	Yes
n-hexacosane	C26	Yes	Yes
n-heptacosane	C27	Yes	Yes
n-octacosane	C28	Yes	Yes
n-nonacosane	C29	Yes	Yes
n-Triacontane	C30	Yes	Yes
n-hentriacontane	C31	Yes	Yes
n-dotriacontane	C32	Yes	Yes
n-tritriacontane	C33	Yes	Yes



Others

levoglucosan	LEVOG	Yes	Yes
palmitic acid	PALMIA	Yes	Yes
stearic acid	STEARA	Yes	Yes
cholesterol	CHOL	Yes	Yes

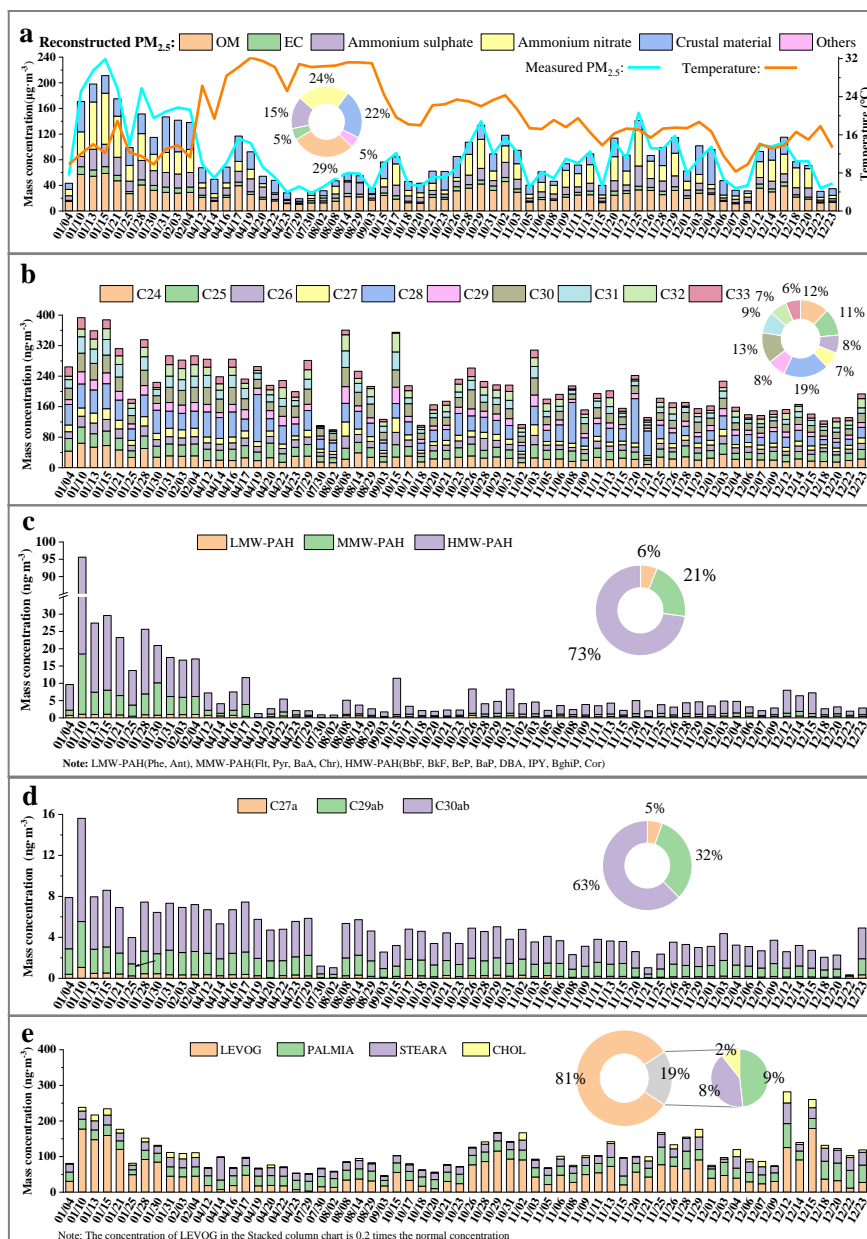
731

732

733



734



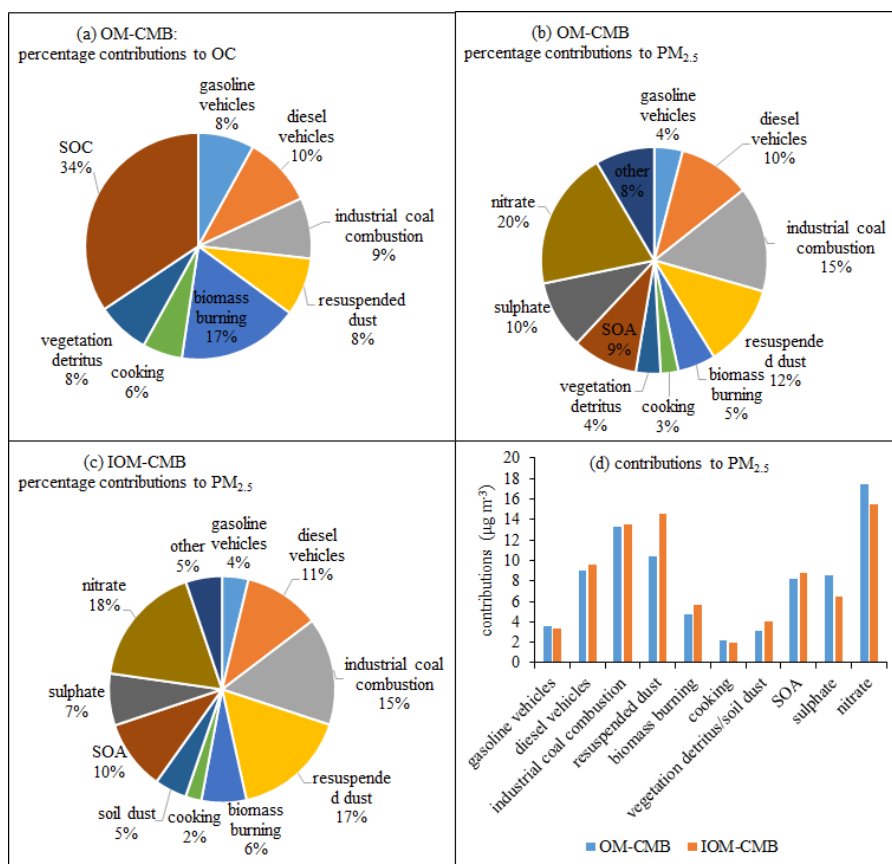
735

736

737

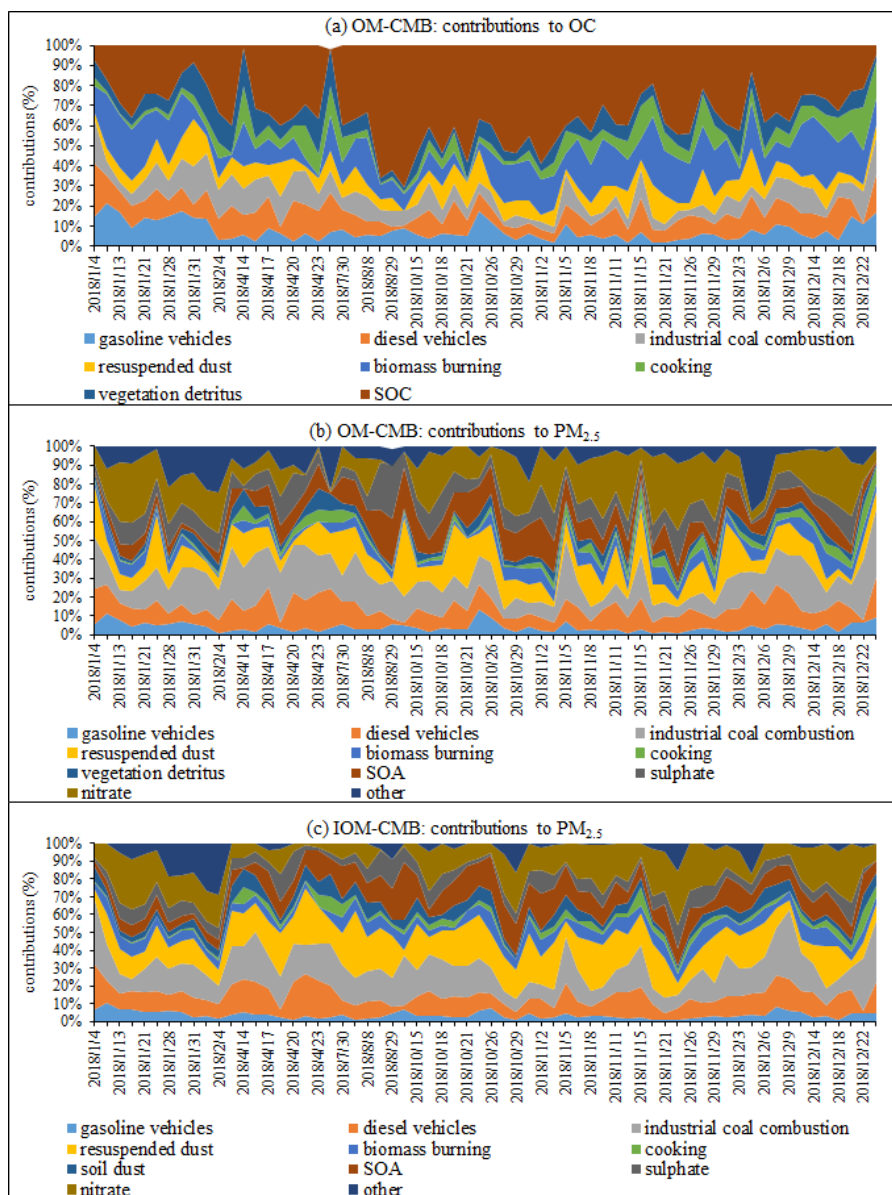
738

Figure 1. The daily concentrations of $PM_{2.5}$, mass closure of main species, and organic components. (a) Mass closure of main species; (b) n-alkanes; (c) PAHs; (d) hopanes; (e) unsaturated fatty acids and cholesterol.



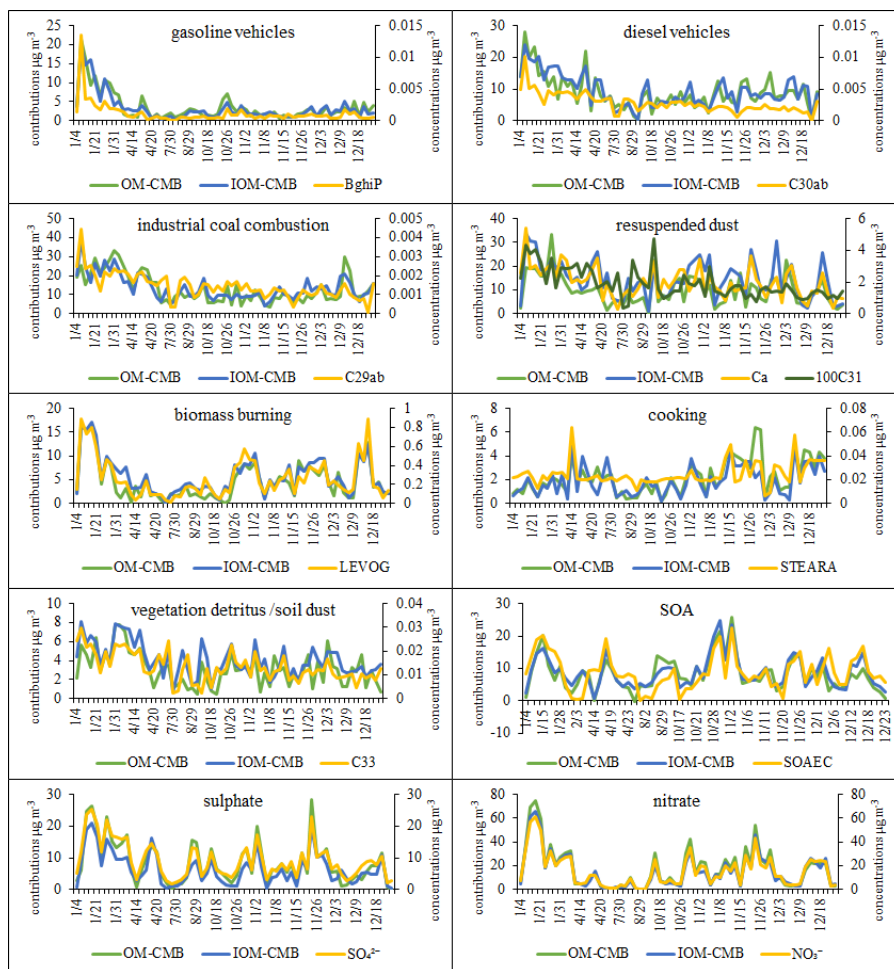
739

740 **Figure 2.** (a) The average of percentage contributions to OC estimated by the OM-CMB; (b) The
741 annual average of percentage contributions to PM_{2.5} estimated by the OM-CMB; (c) The annual
742 average of percentage contributions to PM_{2.5} estimated by the IOM-CMB; (d) Comparison of
743 contributions to PM_{2.5} estimated by the OM-CMB and IOM-CMB.
744



745
746
747
748

Figure 3. (a) Daily contributions to OC estimated by the OM-CMB; (b) Daily contributions to $PM_{2.5}$ estimated by the OM-CMB; (c) Daily contributions to $PM_{2.5}$ estimated by the IOM-CMB.



749

750

Figure 4. Comparisons among source contributions estimated by the OM-CMB and IOM-CMB, and corresponding markers.

751

752